08

Electrophysical properties of thin films of holey graphene functionalized with carbonyl groups

© *P.V. Barkov,*[1] *M.M. Slepchenkov,*[1] *O.E. Glukhova*[1,2]

[1] Saratov National Research State University,
410012 Saratov, Russia
[2] I.M. Sechenov First Moscow State Medical University,
119435 Moscow, Russia
e-mail: barkovssu@mail.ru

Received January 24, 2024
Revised January 24, 2024
Accepted January 24, 2024

Using the density functional theory based tight binding method, we have studied the effect of carbonyl groups on the electrophysical properties of thin films of holey graphene with almost circular holes with a diameter of 1.2 nm and a neck width of 0.7−2 nm. The landing of functional groups was carried out on atoms at the edges of the hole based on an analysis of the map of partial charge distributions according to Mulliken. The phenomenon of charge transfer from carbonyl groups to holey graphene during their interaction has been established. Regularities of changes in the specific electrical conductivity of the films under study with increasing neck width in the „zigzag" direction and in the „armchair" direction of the hexagonal graphene lattice have been revealed. It was shown that the electrical conductivity changes abruptly in the „zigzag" direction and demonstrates a close to linear increase in the „armchair" direction. The presence of anisotropy of electrical conductivity in films of holey graphene was discovered when choosing the direction of quantum electron transport.

Keywords: electrical conductivity, density functional theory based tight binding method, neck width, partial charge, anisotropy.

Introduction

Currently, a new structural derivative of graphene, called perforated graphene is a subject of many theoretical and experimental studies [1–7]. It is a graphene monolayer with nanoscale holes arranged both regularly and irregularly, at some distance from each other (from ~ 1 nm to several μm). Thin films of perforated graphene are semiconductors with the ability to control the band gap by controlling the periodicity and shape of the holes [8]. There are several topological types of perforated graphene structures: perforated graphene structures with almost round, triangular, rectangular holes [9–13] and arbitrary shape holes [14–17]. The most frequently synthesized perforated graphene films are perforated graphene films with round holes and arbitrary shape holes. It was shown in Ref. [9] using a density functional theory (DFT) method, that perforated graphene films with round holes are characterized by the largest energy gap compared to perforated graphene films with triangular and rectangular holes. The advantages of perforated graphene films with round holes include high mechanical stability that was previously determined [18] and isotropic elastic properties [19]. Moreover, nanotubes of various chirality [20,21] can be grown on the basis of perforated graphene structures with round holes. For instance, it was previously shown that the growth of single-walled carbon nanotubes (SWCNT) (6.6) and (9.9) is energetically beneficial in round holes with a size of $\sim 0.8-1.2$ nm [22,23].

Perforated graphene is commonly used in various applications due to its unique properties. Field-effect transistors are already manufactured on the basis of perforated graphene structures, ensuring a current almost 100 times greater than similar devices based on graphene nanoribbons [24]. Perforated graphene is a promising material for the production of electrodes for supercapacitors and lithium ion batteries, since the presence of holes facilitates the free penetration of lithium ions into the electrode [25–27]. The porous structure of perforated graphene allows it to be used for production of highly efficient membranes for separating various gases in mixtures [28] and for water purification [29–31]. The perforated graphene has some unique physical and chemical properties in addition to the advantages already listed, due to the modification of the edge atoms of the holes by attaching various functional groups to them, such as carboxyl groups COOH, amine groups NH_2, hydroxyl groups OH, as well as the oxygen atoms, hydrogen, etc. Modification of the edges of the holes results in a significant expansion of the range of functional applications of perforated graphene, and for this reason such modification is called functionalization.

The purpose of this study is to identify patterns of the effect of functionalization by carbonyl (C=O) groups on the electrophysical properties of thin films of perforated graphene with almost round holes with a diameter of 1.2 nm from the perspective of analyzing the prospects for the potential use of such films as a sensitive element in sensors. Perforated graphene films with almost round holes with a

diameter of 1.2 nm and a neck width varying in the range of 0.7−2nm are the subjects of the study.

1. Research methods

The study was conducted using the density functional theory method in the approximation of self-consistent-charge density-functional tight-binding (SCC DFTB) [32] using the software package DFTB+ [33,34]. The method and the software package used have previously been widely tested in the studies of the atomic structure, electronic and electrophysical properties of carbon nanomaterials of various topologies [35]. The SCC DFTB method is chosen also due to the polyatomic nature of the calculated supercells, which contain several hundred atoms. The electrophysical characteristics of the studied films were calculated in the full basis (s- and p-electronic orbitals). The equilibrium atomic configuration of thin film supercells within the framework of optimization was searched until the values of interatomic forces became less than $10^{-4}\,\mathrm{eV}\cdot\mathrm{\AA}^{-1}$. The reverse space was partitioned according to the Monkhorst−Pack scheme [36] using a mesh of k-points of size $4\times4\times1$ for optimization of the atomic structure of supercells.

The electrical conductivity of the studied structures was calculated within the framework of the Landauer−Butticker formalism [37] according to the following formula

$$G = 2e^2/h \int_{-\infty}^{\infty} T(E)F_T(E-E_\mathrm{F})dE, \qquad (1)$$

where $T(E)$ — the average electron transmission function, E_F — the Fermi level of the electrodes, e^2/h — the quantum of conductivity, F_T — the function of thermal broadening of energy levels, defined as

$$F_T = \frac{1}{4k_\mathrm{B}T}\,\mathrm{sech}^2\left(\frac{E-E_\mathrm{F}}{2k_\mathrm{B}T}\right). \qquad (2)$$

The coefficient 2 before the integral takes into account spin. The electron transmission function $T(E,k)$ is expressed as follows

$$T(E,k) = Tr\left(\Gamma_S(E,k)G_C^A(E,k)\Gamma_D(E,k)G_C^R(E,k)\right), \quad (3)$$

where $G_C^A(E,k)$ and $G_C^R(E,k)$ — leading and lagging Green's matrices describing the interaction of the simulated system with electrodes, and $\Gamma_S(E,k)$ and $\Gamma_D(E,k)$ — expansion matrices of electronic states of the source and drain electrodes. All calculations were performed with $T = 300\,\mathrm{K}$.

2. Atomic structure of supercell films of perforated graphene

The initial supercell of the perforated graphene film had dimensions 2.46×2.55 nm (along axes X and Y) and contained 186 carbon atoms (Fig. 1, a). Almost round hole in the center of the supercell has a diameter of ~ 1.2 nm. The minimum distance between two adjacent holes in the periodic structure of the film, referred as the neck width, was 0.74 nm in the direction of „zigzag“ (axes X) and 0.99 nm in the direction of „armchair“ (axis Y). These metric parameters were chosen taking into account experimental data on the synthesis of perforated graphene, according to which the most commonly synthesized structures of perforated graphene have a hole diameter in the range 1−5 nm [38] and a neck width of 0.6−1.2 nm [39]. A certain set of statistical calculation data was required for defining the relationship between the atomic structure and the electrophysical properties of the studied nanomaterial, and therefore 10 supercells of perforated graphene films were constructed, differing in neck width along the direction „zigzag“ (W_X) and along the direction „armchair“ (W_Y) (fig. 1, b). The supercells were built using to the following principle: 1) the width of the neck W_X varied from 0.74 to 2.22 nm in increments of $\Delta W_X = 0.24$ nm, while the neck width W_Y remained equal to 0.99 nm; 2) the neck width W_Y varied from 0.99 to 2.27 nm in increments of $\Delta W_Y = 0.42$ nm, while the neck width W_X remained equal to 0.74 nm.

3. Step-by-step functionalization of perforated graphene films by carbonyl groups

The process of step-by-step functionalization of perforated graphene films in C=O groups was modelled using an original algorithm for attaching functional groups to the edge atoms of the hole [40]. The functional groups were attached precisely at the edges of the hole, since unsaturated carbon bonds are present in this area, which means that the edge atoms have greater reactivity. The attachment point for each subsequent C=O group was chosen based on the analysis of the electron density distribution over the atoms of the perforated graphene supercell. It is known that it is the atoms with the largest excess charge that act as active centers during the formation of covalent bonds with absorbent chemical compounds. Therefore, at each step of functionalization, the C=O group was attached to the atom with the largest excess negative charge. Mulliken partial charge distribution map was calculated for the atoms of the initial supercell (Fig. 2, a) for the attachment of the first functional group and the edge atom of the hole with the largest excess charge was determined according to this map. The neighboring atoms were saturated with hydrogen atoms for avoiding the formation of unnecessary covalent bonds between the C=O group and carbon atoms, which are the nearest neighbors of the atom on which the functional group sat. After that, the equilibrium atomic configuration of the supercell was searched by varying the coordinates of all the atoms of the supercell, and then a new map of Mulliken partial charges was calculated (Fig. 2, b).

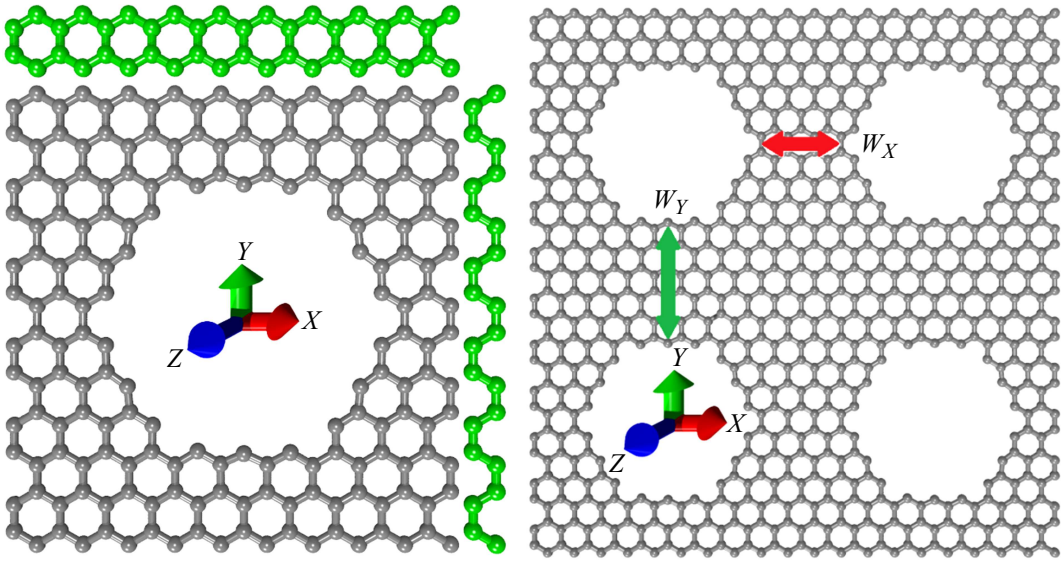

Figure 1. Supercell of perforated graphene with the minimum possible step of increase of the neck width in the directions „zigzag“ (ΔW_X) and „armchair“ (ΔW_Y) (a); the width of the neck along the direction „zigzag“ (W_X) and along the direction „armchair“ (W_Y) (b).

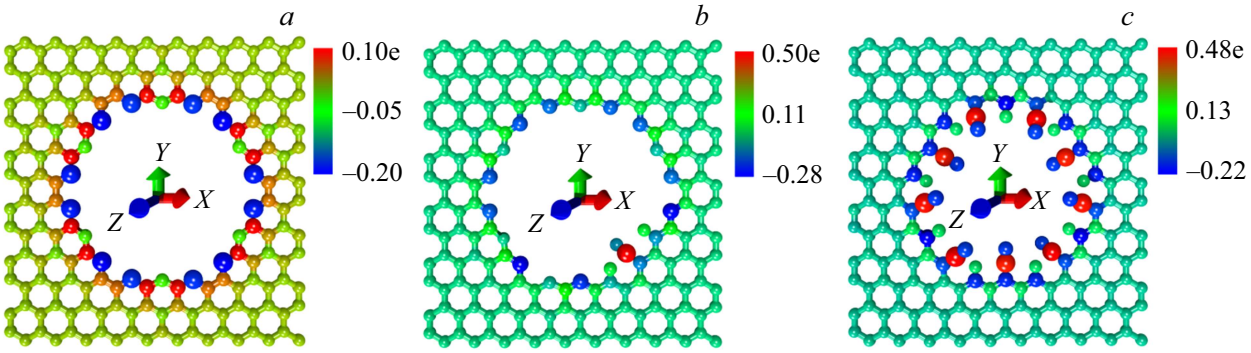

Figure 2. Maps of Mulliken partial charge distributions for supercell atoms of perforated graphene during step-by-step functionalization with C=O-groups: without C=O-groups (a); with one C=O-group (b); with nine C=O-groups (c). The color scale shows the value of the partial charge.

Further, the following C=O groups were joined step by step according to the algorithm described above. The complete saturation of the edge atoms of the hole of the considered supercell of perforated graphene was achieved by joining nine C=O groups. The partial charge distribution pattern for this case is shown in Fig. 2, c. The analysis of the calculated distributions showed that the attached C=O groups give charge to the atoms of perforated graphene, and the total value of the given charge was 2.51 e.

It was important to ensure the energy efficiency of the process of attachment of each subsequent C=O group during the step-by-step functionalization of perforated graphene which means that the studied object retains its structural stability. For this reason the value of the energy of formation of ΔH_f was calculated at each step of functionalization using the following formula:

$$\Delta H_f = E_{G+n\,\mathrm{C{=}O}+m\mathrm{H}} - E_G - E_{n\,\mathrm{C{=}O}} - E_{m\mathrm{H}}, \qquad (4)$$

where $E_{G+n\mathrm{C{=}O}+m\mathrm{H}}$ — the energy of a supercell of perforated graphene with planted groups C=O (n — the number of C=O groups) and attached hydrogen atoms (m — number of hydrogen atoms planted), E_G — energy of perforated graphene in the absence of functional groups, $E_{n\mathrm{C{=}O}}$ — energy of C=O groups, $E_{m\mathrm{H}}$ — hydrogen atoms. The values of ΔH_f at different stages of functionalization range from -1.6 to -12.8 eV according to the calculated data. Negative values of ΔH_f indicate the energy stability of the considered configuration of the atomic structure.

4. Electrophysical properties of perforated graphene films with carbonyl groups

The impact of carbonyl groups on the electrophysical properties of perforated graphene films was estimated by

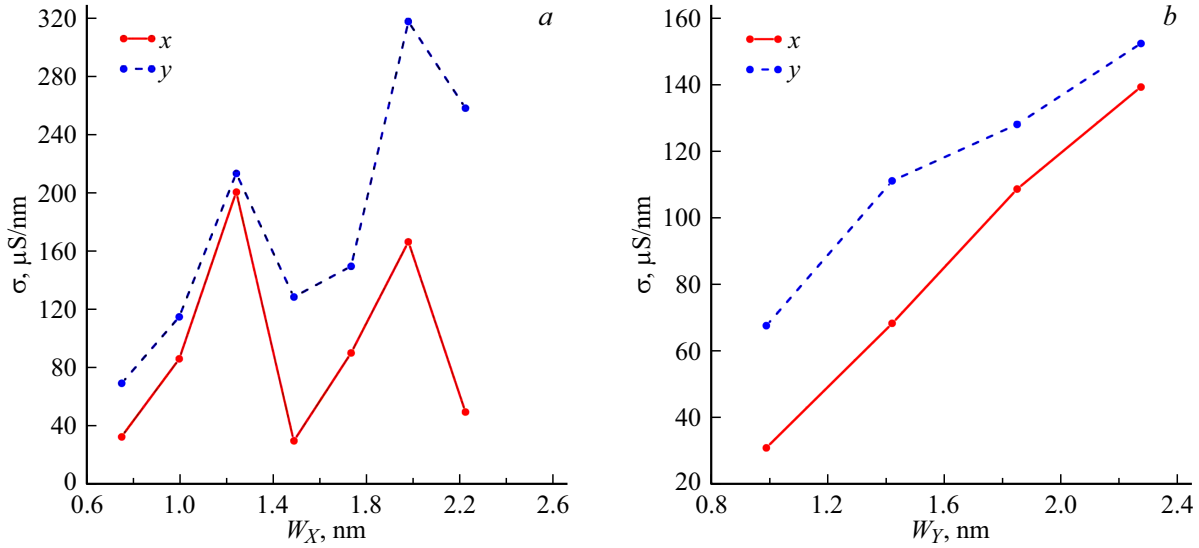

Figure 3. Graphs of the dependence of the conductivity of perforated graphene functionalized by carbonyl groups on the width of the neck as it increases along the „zigzag“ (a) and „armchair“ (b) direction.

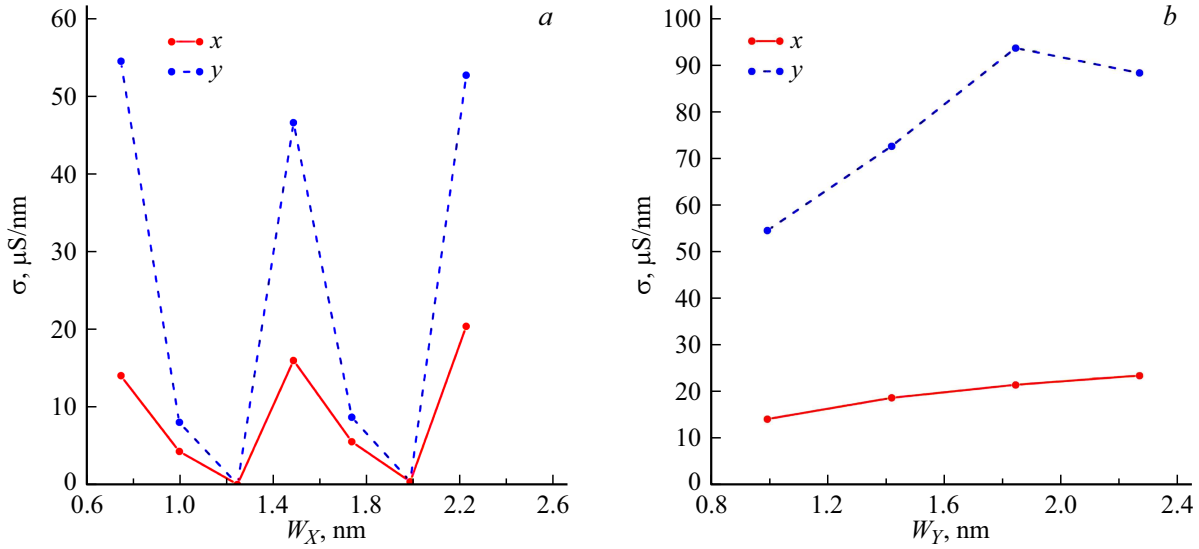

Figure 4. Graphs of the dependence of the conductivity of nonfunctionalized perforated graphene on the width of the neck when it increases along the „zigzag“ (a) and „armchair“ (b) direction.

the magnitude of the conductivity. The conductivity was calculated for two directions of quantum electron transport in the studied films: along the direction „zigzag“ (axis X) and along the direction „armchair“ (axis Y) of the hexagonal graphene lattice. The conductivity values σ of perforated graphene films with fully saturated C=O-group atoms along the edges of the hole calculated for two directions of electron transport are shown in Fig. 3 for different values of the neck width W_X and W_Y. Figure 4 shows for comparison the dependences of the conductivity σ on the neck width (W_X and W_Y) for films of nonfunctionalized perforated graphene. The analysis of the graphs in Fig. 3, a shows that the conductivity changes abruptly in both directions of electron transport with an increase of the neck width along the „zigzag“ hexagonal lattice of graphene. The step of the jumps is equal to three, i.e. maximum conductivity values are observed with values of neck width $W_X = 1.23$ and 1.97 nm. For the same values of the neck width, the conductivity in case of the current transfer along the direction „armchair“ is greater than along the direction „zigzag“, and differences of values σ become 2–3-fold with the increase of W_X. Fig. 3, b shows that the conductivity does not change abruptly with an increase of the neck width along the direction „armchair“ but demonstrates an increase close to linear in both directions of electron transport. The values of σ are greater in the „armchair“ direction than in the „zigzag“ direction, and the difference is 2-fold at values $W_Y = 0.99$ and 1.42 nm and the difference is 0.93 times with

Values of the Fermi level of a perforated graphene (PG) film functionalized by C=O groups

The stages of functionalization of perforated graphene	E_F, eV
0: Nonfunctionalized perforated graphene	−5.25
1: PG + 1C=O + 2H	−5.04
2: PG + 2C=O + 4H	−4.98
3: PG + 3C=O + 4H	−4.91
4: PG + 4C=O + 5H	−4.68
5: PG + 5C=O + 7H	−4.46
6: PG + 6C=O + 7H	−4.40
7: PG + 7C=O + 8H	−4.26
8: PG + 8C=O + 9H	−4.12
9: PG + 9C=O + 9H	−4.06

$W_Y = 2.22$ nm. In general, it can be said that an anisotropy of conductivity is present in films of perforated graphene functionalized by carbonyl groups. It is possible to draw the following conclusions comparing the conductivity graphs in Fig. 3 and 4:

1) The anisotropy of the perforated graphene electrical conductivity is characteristic of both functionalized and non-functionalized perforated graphene.

2) The abrupt behavior of the value σ with an increase of the neck width W_X occurs regardless of whether the perforated graphene is functionalized by C =O groups or not. At the same time, the order of alternating maxima and minima of the magnitude of σ changes when carbonyl groups are added.

3) The patterns of change of the magnitude of σ with an increase of the neck width W_Y of nonfunctionalized and functionalized perforated graphene are similar. At the same time, the difference in values of σ between the directions of electron transport in the presence of C=O groups becomes smaller.

4) Functionalization by C=O-groups results in an increase of the conductivity of perforated graphene several times compared to the original non-functionalized configuration.

The above-mentioned changes of the electrical conductivity of perforated graphene in case of attachment of C=O groups to atoms at the edges of the hole can be explained by the following reasons:

1) Perforated graphene films receive a charge from functional groups, which changes the position of the Fermi level, as clearly demonstrated by the data in the table. The displacement of Fermi level by more than 1 eV towards the conduction band results in noticeable changes of conductivity since the electronic states precisely near the Fermi level E_F are the main contributors to the electron transmission function.

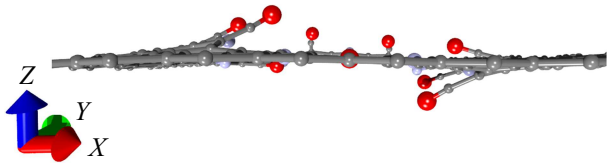

Figure 5. A supercell of a perforated graphene film functionalized by nine C=O groups (side view).

2) The position of the edge atoms of the hole in the basal plane changes after the addition of C=O groups as a result of optimization of the atomic structure of the supercell of perforated graphene. Fig. 5 shows that the carbon atoms along the edges of the hole to which the functional groups are attached are no longer located in the basal plane, but either above or below it, which suggests a change of the valence and dihedral angles between the corresponding C−C bonds.

Conclusion

In summary, the following patterns were defined based on the results of SCC DFTB calculations. The functionalization of atoms along the edges of the hole of perforated graphene by C=O-groups results in the redistribution of the electronic charge in the system „perforated graphene + C=O groups“, as a result of which a significant part of the charge passes to the carbon atoms of graphene from the functional groups. The electronic structure of perforated graphene significantly changes because of the received charge which is manifested by the displacement of the Fermi level in the direction of the conduction band by more than 1 eV. Perforated graphene functionalized by C=O groups is characterized by an abrupt change of the conductivity with an increase of the neck width in „zigzag“ direction of hexagonal graphene lattice, which is also characteristic of nonfunctionalized graphene. At the same time, the order of alternating minima and maxima of conductivity changes when functional groups are attached because of the above-described changes of the electronic structure of perforated graphene and distortion of its hexagonal lattice near the hole. The conductivity anisotropy is inherent in both nonfunctionalized and functionalized perforated graphene. It is possible to assume that perforated graphene films functionalized by carbonyl groups will be a promising material for manufacturing of highly sensitive sensors.

Funding

The work was supported by a grant from the Russian Science Foundation (project №23-72-01122, https://rscf.ru/project/23-72-01122/).

Conflict of interest

The authors declare that they have no conflict of interest.

References

[1] Y. Lin, Y. Liao, Zh. Chen, J.W. Connell. Mater. Res. Lett., **5**, 209 (2017). DOI: 10.1080/21663831.2016.1271047

[2] J. Bai, X. Zhong, S. Jiang, X. Duan. Nature Nanotechnol., **5**, 190 (2010). DOI: 10.1038/nnano.2010.8

[3] M. Kim, N.S. Safron, E. Han, M.S. Arnold, P. Gopalan. Nano Lett., **10**, 1125 (2010). DOI: 10.1021/nl9032318

[4] T.H. Han, Y.-K. Huang, A.T.L. Tan, V.P. Dravid, J. Huang. J. American Chem. Society, **133**, 15264 (2011). DOI: 10.1021/ja205693t

[5] X. Zhao, C.M. Hayner, M.C. Kung, H.H. Kung. Adv. Energy Mater., **1**, 1079 (2011). DOI: 10.1002/aenm.201100426

[6] X. Han, M.R. Funk, F. Shen, Y.-C. Chen, Y. Li, C.J. Campbell, J. Dai, X. Yang, J.-W. Kim, Y. Liao, J.W. Connell, V. Barone, Z. Chen, Y. Lin, L. Hu. ACS Nano, **8**, 8255 (2014). DOI: 10.1021/nn502635y

[7] Y. Xu, Z. Lin, X. Zhong, X. Huang, N.O. Weiss, Y. Huang, X. Duan. Nature Commun., **5**, 4554 (2014). DOI: 10.1038/ncomms5554

[8] H. Sahin, S. Ciraci. Phys. Rev. B, **84**, 035452 (2011). DOI: 10.1103/PhysRevB.84.035452

[9] G. Tang, Z. Zhang, X. Deng, Z. Fan, Y. Zeng, J. Zhou. Carbon, **76**, 348 (2014). DOI: 10.1016/j.carbon.2014.04.086

[10] J. Zhang, W. Zhang, T. Ragab, C. Basaran. Comput. Mater. Sci., **153**, 64 (2018). DOI: 10.1016/j.commatsci.2018.06.026

[11] A. Kausar. Polym.-Plast. Technol. Mater., **58**, 803 (2019). DOI: 10.1080/25740881.2018.1563111

[12] M. Yarifard, J. Davoodi, H. Rafii-Tabar. Comput. Mater. Sci., **111**, 247 (2016). DOI: 10.1016/j.commatsci.2015.09.033

[13] H.X. Yang, M. Chshiev, D.W. Boukhvalov, X. Waintal, S. Roche. Phys. Rev. B., **84**, 214404 (2011). DOI: 10.1103/PhysRevB.84.214404

[14] M.K. Rabchinskii, A.S. Varezhnikov, V.V. Sysoev, M.A. Solomatin, S.A. Ryzhkov, M.V. Baidakova, D.Yu. Stolyarova, V.V. Shnitov, S.S. Pavlov, D.A. Kirilenko, A.V. Shvidchenko, E.Yu. Lobanova, M.V. Gudkov, D.A. Smirnov, V.A. Kislenko, S.V. Pavlov, S.A. Kislenko, N.S. Struchkov, I.I. Bobrinetskiy, A.V. Emelianov, P. Liang, Z. Liu, P.N. Brunkov. Carbon, **172**, 236 (2021). DOI: 10.1016/j.carbon.2020.09.087

[15] S.A. Ryzhkov, M.K. Rabchinskii, V.V. Shnitov, M.V. Baidakova, S.I. Pavlov, D.A. Kirilenko, P.N. Brunkov. J. Phys. Conf. Ser., **1695**, 012008 (2020). DOI: 10.1088/1742-6596/1695/1/012008

[16] M.K. Rabchinskii, S.D. Saveliev, D.Yu. Stolyarova, M. Brzhezinskaya, D.A. Kirilenko, M.V. Baidakova, S.A. Ryzhkov, V.V. Shnitov, V.V. Sysoev, P.N. Brunkov. Carbon, **182**, 593 (2021). DOI: 10.1016/j.carbon.2021.06.057

[17] V.V. Shnitov, M.K. Rabchinskii, M. Brzhezinskaya, D.Yu. Stolyarova, S.V. Pavlov, M.V. Baidakova, A.V. Shvidchenko, V.A. Kislenko, S.A. Kislenko, P.N. Brunkov. Small, **17**, 2104316 (2021). DOI: 10.1002/smll.202104316

[18] A. Winter, Y. Ekinci, A. Gölzhäuser, A. Turchanin. 2D Materials, **6**, 021002 (2019). DOI: 10.1088/2053-1583/ab0014

[19] C. Carpenter, A.M. Christmann, L. Hu, I. Fampiou, A.R. Muniz, A. Ramasubramaniam, D. Maroudas. Appl. Phys. Lett., **104**, 141911 (2014). DOI: 10.1063/1.4871304

[20] J. Park, V. Prakash. J. Appl. Phys., **116**, 014303 (2014). DOI: 10.1063/1.4885055

[21] H.-J. Qian, G. Eres, S. Irle. Molecular Simulation, **43**, 1269 (2017). DOI: 10.1080/08927022.2017.1328555

[22] M.M. Slepchenkov, D.S. Shmygin, G. Zhang, O.E. Glukhova. Carbon, **165**, 139 (2020). DOI: 10.1016/j.carbon.2020.04.069

[23] V.V. Shunaev, O.E. Glukhova. Materials, **13**, 5219 (2020). DOI: 10.3390/ma13225219

[24] W. Shim, Y. Kwon, S. Jeon, W.-R. Yu. Scientific Reports, **5**, 16568 (2015). DOI: 10.1038/srep16568

[25] Y. Lin, X. Han, C.J. Campbell, J.-W. Kim, B. Zhao, W. Luo, J. Dai, L. Hu, J.W. Connell. Adv. Functional Mater., **25**, 2920 (2015). DOI: 10.1002/adfm.201500321

[26] Y-Y. Peng, Y.-M. Liu, J.-K. Chang, C-H. Wu, M.-D. Ger, N.-W. Pu, C.-L. Chang. Carbon, **81**, 347 (2015). DOI: 10.1016/j.carbon.2014.09.067

[27] C.-H. Yang, P.-L. Huang, X.-F. Luo, C.-H. Wang, C. Li, Y.-H. Wu, J.-K. Chang. Chem. Sus. Chem., **8**, 1779 (2015). DOI: 10.1002/cssc.201500030

[28] S.P. Koenig, L. Wang, J. Pellegrino, J.S. Bunch. Nature Nanotechnol., **7**, 728 (2012). DOI: 10.1038/nnano.2012.162

[29] D. Cohen-Tanugi, J.C. Grossman. Nano Lett., **12**, 3602 (2012). DOI: 10.1021/nl3012853

[30] S.C. O'Hern, D. Jang, S. Bose, J.-C. Idrobo, Y. Song, T. Laoui, J. Kong, R. Karnik. Nano Lett., **15**, 3254 (2015). DOI: 10.1021/acs.nanolett.5b00456

[31] S.P. Surwade, S.N. Smirnov, I.V. Vlassiouk, R.R. Unocic, G.M. Veith, S. Dai, S.M. Mahurin. Nature Nanotechnol., **10**, 459 (2015). DOI: 10.1038/nnano.2015.37

[32] M. Elstner, D. Porezag, G. Jungnickel, J. Elsner, M. Haugk, Th. Frauenheim, S. Suhai, G. Seifert. Phys. Rev. B, **58**, 7260 (1998). DOI: 10.1103/PhysRevB.58.7260

[33] B. Aradi, B. Hourahine, Th. Frauenheim. J. Phys. Chem. A, **111**, 5678 (2007). DOI: 10.1021/jp070186p

[34] B. Hourahine, B. Aradi, V. Blum, F. Bonafé, A. Buccheri, C. Camacho, C. Cevallos, M.Y. Deshaye, T. Dumitrică, A. Dominguez, S. Ehlert, M. Elstner, T. van der Heide, J. Hermann, S. Irle, J.J. Kranz, C. Köhler, T. Kowalczyk, T. Kubař, I.S. Lee, V. Lutsker, R.J. Maurer, S.K. Min, I. Mitchell, C. Negre, T.A. Niehaus, A.M.N. Niklasson, A.J. Page, A. Pecchia, G. Penazzi, M.P. Persson, J. Řezáč, C.G. Sánchez, M. Sternberg, M. Stöhr, F. Stuckenberg, A. Tkatchenko, V.W.-Z. Yu, T. Frauenheim. J. Chem. Phys., **152**, 20 (2020). DOI: 10.1063/1.5143190

[35] M. Elstner, G. Seifert. Philos. Trans. R. Soc. A, **372**, 20120483 (2014). DOI: 10.1098/rsta.2012.0483

[36] H.J. Monkhorst, J.D. Pack. Phys. Rev. B, **13**, 5188 (1976). DOI: 10.1103/PhysRevB.13.5188

[37] S. Datta. *Quantum Transport: Atom to Transistor* (Cambridge University Press: Cambridge, London, UK, 2005), p. 404.

[38] M.K. Rabchinskii, V.V. Shnitov, A.T. Dideikin, A.E. Aleksenskii, S.P. Vul, M.V. Baidakova, I.I. Pronin, D.A. Kirilenko, P.N. Brunkov, J. Weise, S.L. Molodtsov. J. Phys. Chem. C, **12**, 28261 (2016). DOI: 10.1021/acs.jpcc.6b08758

[39] B. Sakkaki, H.R. Saghai, G. Darvish, M. Khatir. Opt. Mater., **122**, 111707 (2021). DOI: 10.1016/j.optmat.2021.111707

[40] O.E. Glukhova, P.V. Barkov. Lett. Mater., **12**, 392 (2021). DOI: 10.22226/2410-3535-2021-4-392-396

Translated by A.Akhtyamov